

Statistics of cluster multiplicity and the nature of UHE cosmic ray sources

Diego Harari, Silvia Mollerach and Esteban Roulet
CONICET, Centro Atómico Bariloche,
Av. Bustillo 9500, Bariloche, 8400, Argentina.

January 13, 2019

Abstract

We study in detail the properties of clusters of ultra high energy cosmic ray events, looking in particular to their angular correlation function, to the relative frequency of clusters with different multiplicities (e.g. doublets vs. triplets or quadruplets), as well as the way in which these quantities should evolve for different ultra high energy cosmic rays source scenarios as a function of the experimental exposure achieved. We identify some useful tools which can help to characterise the nature of the cosmic ray sources in a more precise way after a modest increase in statistics will be achieved in the very near future, even before strong signals from individual sources become eventually observable.

1 Introduction

In spite of the big effort done over the last decades to unravel the origin and nature of the cosmic rays (CRs) at ultra high energies (UHE), most of the relevant questions related to them remain still unanswered [1]. Certainly the main obstacle has been the scarcity of data, which is due to the smallness of the fluxes at the highest energies (e.g. $\sim 1/\text{km}^2\text{yr}$ for $E > 10^{19}$ eV). The observed isotropy of CRs above the ankle (i.e. for $E > 5 \times 10^{18}$ eV), suggests that at these energies CRs are of extragalactic origin, but the nature of these particles (whether they are protons, heavier nuclei, photons or even neutrinos with stronger interactions), the nature of their sources (e.g. steady ones like active galactic nuclei jets, transient ones like gamma ray burst (GRBs) or diffuse ones like decaying topological defects) and the mechanism responsible for their acceleration in bottom-up scenarios or production in top-down ones (and hence the original source spectra) are all under strong debate. All these questions are further challenged by the (lack of) observation of the theoretically expected GZK suppression above $\sim 6 \times 10^{19}$ eV, due to the attenuation that CR

protons coming from far away sources should suffer due to their interactions with CMB photons (or similarly due to the photodisintegration processes that would affect the propagation of heavier nuclei). Clearly a big boost in our understanding of these issues could be obtained if individual CR sources were identified, and this search is indeed the main purpose of the next generation of observatories, like the Pierre Auger one now under completion.

There has been a lot of discussion during the last years about possible hints in the existing data of an excess of clustering in the highest energy range ($E > 4 \times 10^{19}$ eV), that could be already indicating the possible emergence of the first strong CR sources out of a more diffuse background of unresolved sources. This excess clustering (with respect to the expectations from chance coincidences of an isotropic distribution) has been observed by the AGASA group [2](which detected 4 doublets and one triplet within 2.5° , out of a total of 57 events¹) and also in a combined analysis of data from several experiments [3] (Yakutsk, Haverah Park, AGASA and Volcano Ranch, which obtained 8 doublets and 2 triplets within 4° out of a total of 92 events), although it does not seem to be present in Fly's Eye or Hi Res data [4].

In this work we will study in detail the properties of the event clusters expected in different scenarios of UHECR sources, with the aim of devising the most appropriate tools to discriminate among them. The results we obtain suggest that a modest increase in the present statistics (as could be achieved after one year of AUGER observations) will allow to clarify significantly the existing debate, even before any strong (and hence unambiguous) signal from an individual CR source is observed.

2 Clusters from chance coincidences

Before considering the possibility that the clusters are due to strong CR sources with large enough fluxes so as to have induced more than one event with the present experimental exposures, it is important to consider the expected clustering signal from just chance coincidences in the limit in which all events observed were produced by independent sources, which are too weak to produce by themselves an individual cluster (i.e., considering that there is a very large number of sources, all with a small chance of producing even a single event in the present experiments). As we show below, this probability depends strongly on the way the sources are distributed across the sky, and so we start with the simplest case of an isotropic distribution.

2.1 Isotropic sources

A commonly adopted measure of a clustering signal is obtained from the study of the angular correlation of pairs, $dN_p/d\theta$, which gives the number of event pairs with

¹We are not including in our discussion one event with energy slightly below 4×10^{19} eV, included by AGASA because it lead to an extra doublet.

angular separation between θ and $\theta + d\theta$ expected from a total number n of events. In the case of an isotropic distribution, it can be written as

$$\frac{dN_p}{d\theta} \propto \sin \theta \int d\Omega_1 \int d\Omega_2 \omega(\delta_1)\omega(\delta_2) \delta(\hat{\Omega}_1 \cdot \hat{\Omega}_2 - \cos \theta), \quad (1)$$

where $d\Omega_i = \cos \delta_i d\delta_i d\alpha_i$ in terms of declination and right ascension, and δ_i has to be integrated over the declinations observable to the experiment. The normalization is such that the total number of pairs (i.e. integrating over θ) is just $n(n-1)/2$.

The function $\omega(\delta)$ takes into account the declination dependence of the exposure of the experiment under consideration, and for a surface detector² is given by [5]

$$\omega(\delta) \propto \cos b_0 \cos \delta \sin \alpha_m + \alpha_m \sin b_0 \sin \delta, \quad (2)$$

where b_0 is the latitude of the experiment (e.g. $b_0 = 35.8^\circ$ for AGASA) and

$$\alpha_m = \begin{cases} 0 & \xi > 1 \\ \arccos \xi & -1 \leq \xi \leq 1 \\ \pi & \xi < -1 \end{cases} \quad \xi = \frac{\cos \theta_m - \sin b_0 \sin \delta}{\cos b_0 \cos \delta}, \quad (3)$$

with θ_m the maximum zenith angle of the CR showers considered ($\theta_m = 45^\circ$ for the AGASA sample).

Potential point sources of UHECRs should manifest themselves through a significant enhancement above random expectations of the correlation function at values around and below the angular reconstruction accuracy. Energy-dependent deflections of CR trajectories by intervening magnetic fields may disperse the arrival directions, and thus clustering signals may be spread over larger angular scales. It thus proves convenient to analyse the integrated correlation function $N_p(< \theta) = \int_0^\theta d\theta' dN_p/d\theta'$, which is simply the total number of event pairs which are separated by an angle smaller than θ (albeit the most common practice is to look instead at the distribution $dN_p/d\theta$). The number of pairs at angles smaller than θ is plotted in the upper panel in Figure 1, for a total number of 57 events and for the AGASA exposure, and is compared with the AGASA data. The solid line follows the mean value of 10000 simulated isotropic random realizations. The error bars contain 95% of the results in the random realizations at each angular scale (the larger and smaller 2.5% portions were discarded). The points are the AGASA data. An excess of pairs with respect to random expectations is apparent at small angles ($\theta < \text{few degrees}$), which is related to the observation of 4 doublets and one triplet (corresponding to three additional pairs) at separations smaller than 2.5° in the AGASA data, while on average 1.45 doublets would be expected. The probability³ of getting seven or more pairs at $\theta < 2.5^\circ$ in the random realizations is $\sim 1.5 \times 10^{-3}$.

²For the air-fluorescence technique the exposure is more uniform in declination, but has also a dependence on right ascension (see e.g. [4]).

³The significance of these probabilities is a matter of debate [6, 7, 8], given its dependence on the size of the angular bin and the energy threshold.

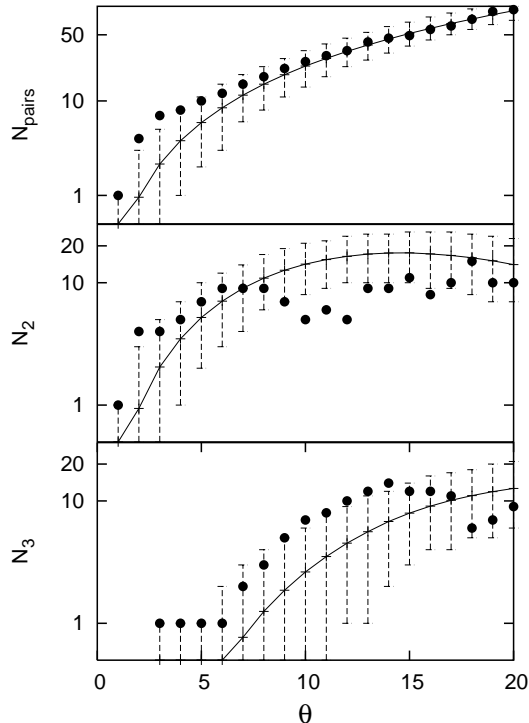


Figure 1: Number of pairs (upper panel), doublets (middle) and triplets (lower) separated by an angle smaller or equal than θ . The solid lines follow the mean of 10000 random realizations of 57 events isotropically distributed with AGASA's exposure. Error bars contain 95% of the results in the simulations. Points correspond to AGASA data above 4×10^{19} eV. Significant departures of the data from random expectations are apparent at angular scales smaller than a few degrees in all three plots, as well as at scales between 9 and 14° in the distribution of doublets and triplets (but not in the number of pairs).

The angular correlation of pairs is the lowest order of a hierarchy of correlation functions. Additional information on the clustering process is encoded, for instance, in the distribution of clusters with different multiplicities. The middle and lower panels in Figure 1 plot respectively the mean number of doublets, $N_2(< \theta)$, and triplets, $N_3(< \theta)$, in random realizations of 57 events with the AGASA exposure, compared with the AGASA data. The excess clustering at small angular scales in AGASA data is noticeable. The probability of forming four doublets at angular scales below 2.5° is ~ 0.06 , and the probability of forming one triplet by chance is ~ 0.016 . The probability of forming 4 doublets and one triplet is of course even smaller than that of forming seven pairs, and is of order $\sim 9 \times 10^{-4}$.

Notice that while the number of event pairs in AGASA data shows no significant departures from isotropic expectations at angular scales larger than a few degrees, their distribution in clusters of different multiplicities deviates noticeably from the

mean at angular scales roughly between 9° and 14° . The number of doublets is in defect and the number of triplets is in excess with respect to random isotropic realizations, at a probability level comparable to the small angular scale clustering signal. Spreading of arrival directions from point UHECR sources by magnetic fields and structure in their spatial distribution are among conceivable causes of such departures. We will come back to a more thorough characterization of this signal in section 4, with alternative statistical tools.

One can get a feeling about the amount of clusters expected for different multiplicities by considering the following simplified model to describe the way clusters are produced by chance coincidences of random isotropic data (a similar approach was adopted in ref. [9] to obtain the probabilities for observations of different numbers of clusters). Let us first ignore the possible effects of a non-uniform exposure, and let us divide the total solid angle Ω monitored by the experiment ($\Omega \simeq 7.2$ sr for AGASA when $\theta_{max} = 45^\circ$ is considered) into N solid angle bins of characteristic size $\Delta\Omega \simeq \pi\theta^2$, so that $N \simeq \Omega/\Delta\Omega \simeq 1050 (\Omega/2\pi)(2.5^\circ/\theta)^2$ for small angles⁴. Now, we start adding events up to a total number n ($n = 57$ for the published AGASA data to which we want to compare), assuming that each event has the same probability ($p = 1/N$) to fall into any of the independent solid angle bins. When two events fall into the same bin, this will then produce a doublet with characteristic separation smaller than θ . It is then simple to show that the average number of clusters $\overline{N}_m(n)$ with a given multiplicity m (e.g. $m = 2$ for doublets, etc.) after observing n events satisfy

$$\overline{N}_m(n+1) = (1-p)\overline{N}_m(n) + p\overline{N}_{m-1}(n) \quad (4)$$

and hence they are just given by a binomial distribution

$$\overline{N}_m(n) = \binom{n}{m} p^{m-1} (1-p)^{n-m}. \quad (5)$$

In particular, one has

$$\overline{N}_1(n) = n \left(1 - \frac{1}{N}\right)^{n-1} \simeq n \exp(-n/N) \quad (6)$$

$$\overline{N}_2(n) = \frac{n(n-1)}{2N} \left(1 - \frac{1}{N}\right)^{n-2} \simeq \frac{n^2}{2N} \exp(-n/N) \quad (7)$$

$$\overline{N}_3(n) = \frac{n(n-1)(n-2)}{6N^2} \left(1 - \frac{1}{N}\right)^{n-3} \simeq \frac{n^3}{6N^2} \exp(-n/N) \quad (8)$$

where the right-most expressions hold for $n \gg 1$. The exponential factors are actually only relevant when the total number of events becomes of the order of the number of available solid angle bins, since in this case most of the events appear in clusters and the multiplicity of the bins rapidly grows suppressing the number of low multiplicity clusters. Clearly by the time this will happen at small angular scales,

⁴ $N = (\Omega/2\pi)/(1 - \cos\theta)$ when θ is not small enough.

the discussion here will be redundant since already the statistics would have become large enough to allow the origin of the observed clustering to be clarified, and hence we will focus the discussion here mainly to the situation in which $n \ll N$. In this case we see that the number of pairs grows quadratically with the number of events observed (and hence with the experimental exposure), the number of triplets grows as the third power and so on, as expected. On the other hand, the ratio between the number of triplets and doublets is $\overline{N}_3(n)/\overline{N}_2(n) \simeq n/3N$, and is hence very small as long as $n \ll N$, as should be the case at present for AGASA.

Hence, a generic prediction of clustering at small angular scales by chance coincidences of an isotropic distribution is that one expects first to see a growing number of doublets ($\propto \mathcal{E}^2$, where \mathcal{E} is the exposure achieved, and of course one expects $n \propto \mathcal{E}$) with no clusters of higher multiplicities (except for very unlikely fluctuations). Then, when the total number of events becomes $\sim (6N^2)^{1/3}$, triplets start to appear with a faster rate of growth ($\propto \mathcal{E}^3$). When this happens the number of doublets is typically $\overline{N}_2 \simeq N^{1/3}$, which is already not a small number. We see then that it is not only surprising to have 4 doublets in the AGASA data when 1.5 ($\sim 57^2/2000$) were expected, but it is probably even more surprising to have observed a triplet out of only 57 events. As an example, we show in Figure 2 the average results obtained from many random isotropic realizations, taking into account a declination dependent exposure like that of AGASA, and plot the resulting number of pairs, doublets, triplets and quadruplets obtained (for $\theta < 2.5^\circ$) as a function of the number of events (solid lines). The main features just mentioned that result from the simple model (dashed lines) are clearly apparent.

The simple model predicts a smaller number of doublets with respect to the Monte Carlo results, what can be understood because the model with solid angle bins requires that each event be assigned to a unique cluster, and thus does not include properly all possible configurations. Consider as an example the case of three events aligned that lead to two doublets but not a triplet⁵. In this case, one of the events participates in two different doublets, but clearly no event can fall in two different angular bins simultaneously. The simple model also predicts an excess (at relatively small n) of triplets and quadruplets with respect to the Montecarlo results. This can be understood because once two events are separated by an angle $< \theta$, to form a triplet the third event has to fall within a solid angle smaller, on average, than $\pi\theta^2$. Hence, the effective number of bins that define the probability of higher multiplicity clusters is larger than the value of N used to calculate the probability of forming doublets. At relatively larger n , when clusters of multiplicity $m + 1$ start to form, the simple model predicts instead a defect of clusters of multiplicity m , for reasons analogous to those that explain the defect in doublets. Notice that this should also affect the probabilities obtained in [9]. The limitations of the simple model appear at smaller values of the number of events n when larger angular separations are considered, since the number of bins N becomes significantly smaller.

⁵Alignment of events can be caused by energy-dependent deflections in magnetic fields, which makes even more relevant to properly discriminate such a clustering signal.

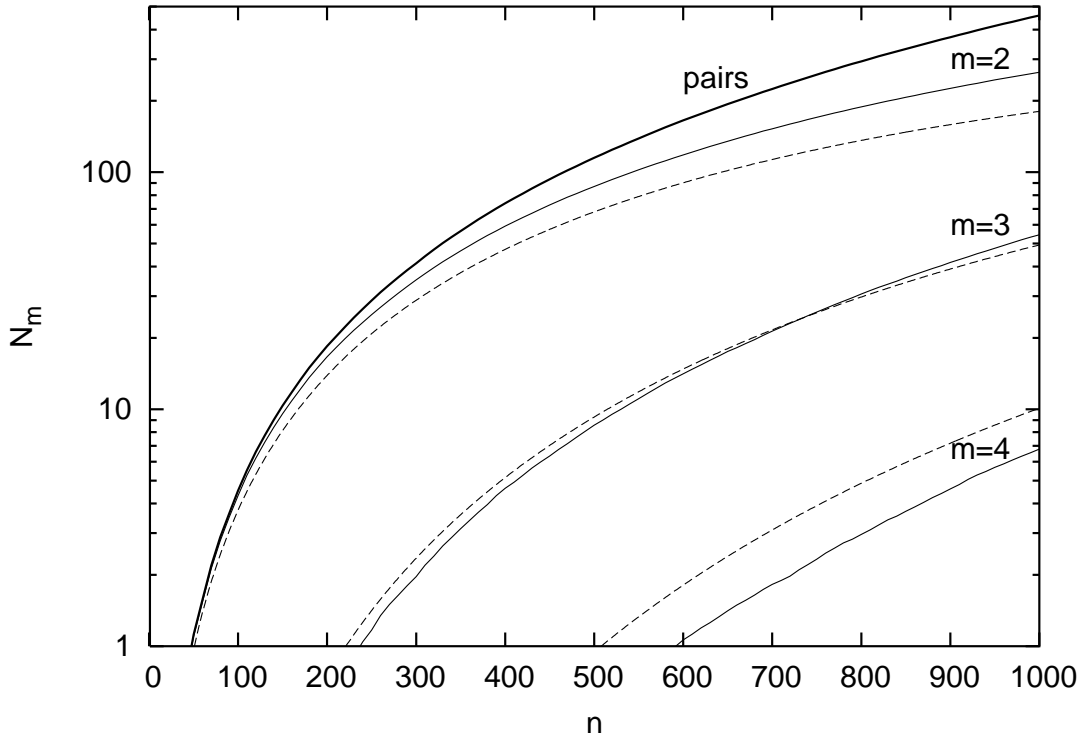


Figure 2: Mean number of pairs (thick solid line), doublets, triplets and quadruplets (thin solid lines) in simulated realizations of n events randomly distributed with AGASA’s declination-dependent exposure. The result of the simple analytic model of eq. (5) for doublets ($m=2$), triplets ($m=3$) and quadruplets ($m=4$) is plotted with dashed lines.

Another property of the multiplets that result from chance coincidences of an isotropic distribution is that, once we take into account that the relative exposure is proportional to $\omega(\delta)$, and hence that the number of observed events should follow $dn/d\delta \propto \omega(\delta) \cos \delta$ (with the $\cos \delta$ factor just from the solid angle associated to δ), the distribution of event pairs on the sky should be proportional to $dN_p \propto \omega(\delta)^2 \cos \delta d\delta$, and similarly the number of triplets (including those in quadruplets and higher multiplets) should behave as $dN_t \propto \omega(\delta)^3 \cos \delta d\delta$, and so on. Hence, the high multiplicity clusters should appear more significantly concentrated at declinations close to the latitude of the experiment, where $\omega(\delta)$ is maximal. This also implies that taking into account the declination dependence of the exposure will slightly enhance the ratio $\overline{N}_3/\overline{N}_2$ (as well as the value of \overline{N}_2 itself) with respect to the estimates done neglecting $\omega(\delta)$. We show in Figure 3 the observed distribution (solid histogram) of events and of event pairs (dashed histogram) in AGASA data, together with the expectations from chance coincidences out of an isotropic distribution. It is clear that although the angular distributions are consistent with the hypothesis of isotropic sources, there is an overall excess in the number of pairs with

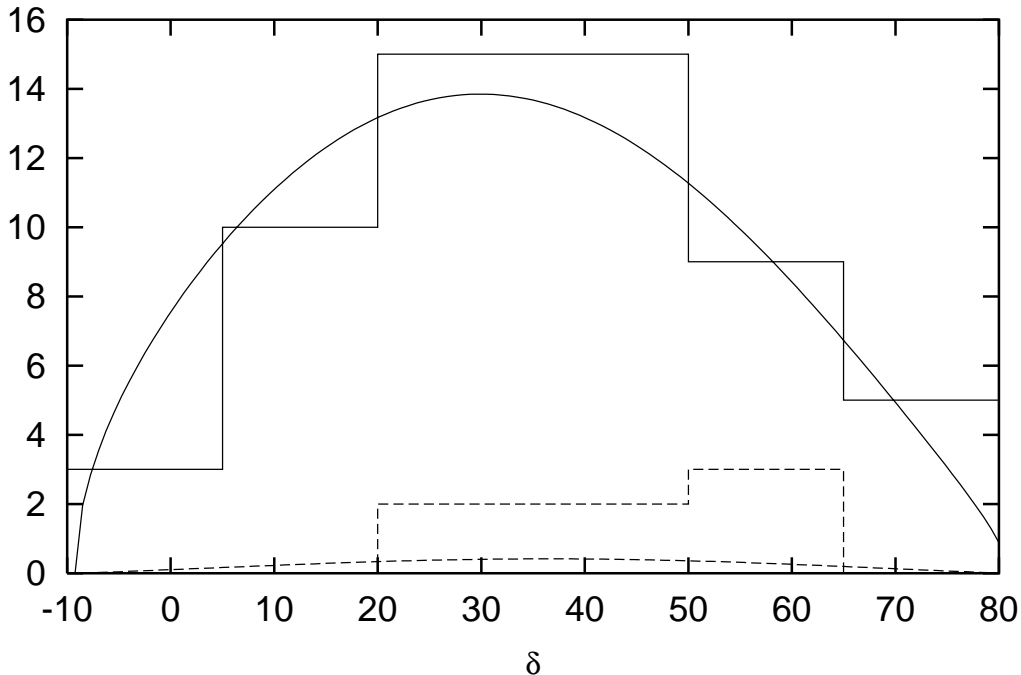


Figure 3: Distribution in declination of AGASA events (solid histogram) and AGASA event pairs (dashed histogram) compared to that expected from chance coincidences of an isotropic distribution with AGASA’s declination dependence of the exposure (solid and dashed curves).

respect to expectations from chance coincidences.

2.2 Structured sources

As is well known, the matter distribution in the local Universe is rather inhomogeneous, specially if we consider the neighbourhood where trans-GZK events may originate (distances < 100 Mpc). In this region indeed large voids are found, and most of the galaxies are distributed on large scale structures like the great attractor, the supergalactic plane, etc., which only cover a relatively small fraction of the sky (see e.g. Figure 10 in [1]). If UHECR sources were to follow a similar distribution, this can have a significant impact on the statistics of the clustering produced by chance overlaps among different sources. For instance, if the sources were distributed uniformly over the sky but ‘avoiding voids’, so that the effective solid angle where sources can be found is smaller than Ω , one could repeat the reasoning of the previous section and find similar expressions but now with a smaller number N' of solid angle bins where clusters could be formed. More generally, if we substitute in the expressions of the previous section $n/\Omega \equiv \rho$, which would be the density

of events per unit solid angle, it is clear that in the limit in which $\rho\Delta\Omega \ll 1$ the generalization of the expression for the number of doublets for the case in which the density of sources is not uniform becomes

$$\overline{N}_2(n) \simeq \frac{\Delta\Omega}{2} \int d\Omega \rho^2 \quad (9)$$

If we now define the average density of events as

$$\overline{\rho} = \frac{1}{\Omega} \int d\Omega \rho \quad (10)$$

we obtain

$$\overline{N}_2(n) \simeq \overline{N}_2^{iso}(n) \langle (\rho/\overline{\rho})^2 \rangle, \quad (11)$$

where

$$\overline{N}_2^{iso}(n) = \frac{\Delta\Omega}{2} \overline{\rho}^2 \Omega \quad (12)$$

is the average number of doublets expected from an isotropic distribution (the \overline{N}_2 computed in the previous section), while

$$\langle (\rho/\overline{\rho})^2 \rangle \equiv \frac{1}{\Omega} \int d\Omega (\rho/\overline{\rho})^2 \quad (13)$$

is a quantity bigger than unity. If one assumes that the distribution of UHECR sources somehow follows the distribution of visible matter, one expects that if the sources are indeed nearby (at least for trans-GZK events) there should be a significant non-uniformity in the arrival directions of the observed events, probably leaving void regions in the sky and with the events finally falling, once larger statistics will be attained, along large scale structures reminiscent to strips across the sky (at these energies, deflections due to magnetic fields are not expected to be large, at least for CR protons). Notice that due to the limited statistics accumulated so far, such a picture is not inconsistent with current observations.

As a simple example, suppose that only a fraction ξ of the observed sky has a uniform distribution of sources, while the rest consists of void regions. This would lead to $\rho = \overline{\rho}/\xi$ in the regions with sources and hence $\langle (\rho/\overline{\rho})^2 \rangle = 1/\xi$, which shows that a significant enhancement in the number of pairs can be achieved by distributing the sources anisotropically. This is understood since in the higher density regions the probability of forming a doublet by chance coincidences is largely enhanced ($\propto \rho^2$). An enhancement in the number of doublets was indeed reported in numerical simulations with a structured source distribution [10]. An even more pronounced effect should also result for the probability of formation of triplets, which can similarly be shown to behave as

$$\overline{N}_3(n) \simeq \overline{N}_3^{iso}(n) \langle (\rho/\overline{\rho})^3 \rangle. \quad (14)$$

3 Clustering from individual sources

The alternative explanation that has been suggested for the observed clustering is that the events in each multiplet originated in the same sources, so that the doublets and triplets observed would correspond to the first manifestations of the brightest sources in the sky. In this scenario, the clusters produced by chance coincidences discussed in the previous section would just be a background for the signal searched, and the excess observed should be attributed to individual sources.

Given a source with a certain flux F (for energies above some specified threshold), the probability that it gives rise to a certain number m of events follows a Poissonian distribution [11]

$$P_m(F) = \frac{\bar{m}^m}{m!} e^{-\bar{m}} \quad (15)$$

where the mean multiplicity is $\bar{m} = F\mathcal{E}$, with \mathcal{E} being the experimental exposure towards the direction of the source (for definiteness we will assume that the exposure is uniform over the whole sky, and just comment later on the effects of non-uniform exposures). Hence, if dn_s/dF denotes the number density of sources leading to a flux between F and $F+dF$, the average number of multiplets expected will be [12]

$$\bar{N}_m = \int_0^\infty dF \frac{dn_s}{dF} P_m(F) \quad (16)$$

On the other hand, the probability of finding k clusters of multiplicity m will also be Poisson distributed, i.e.

$$P_m(k) = \frac{\bar{N}_m^k}{k!} e^{-\bar{N}_m}. \quad (17)$$

Regarding the source distribution function, the simplest situation would be to assume a uniform distribution of sources with similar intrinsic CR luminosities L . In this case, if we further neglect for simplicity the effects of energy losses, the sources leading to a flux larger than F would just be those at a distance closer than $d = \sqrt{L/4\pi F}$, what gives

$$n_s(> F) = \frac{4}{3}\pi\rho_s \left(\frac{L}{4\pi F}\right)^{3/2}, \quad (18)$$

with ρ_s the source volume density. Hence, in this case one finds

$$\frac{dn_s}{dF} \propto F^{-5/2}. \quad (19)$$

Notice that this power law behaviour would lead to a divergent total flux if extrapolated down to very small fluxes (this is nothing else than Olber's paradox), and it is clear that CR attenuation during propagation as well as the effects of the universe expansion and source evolution will ultimately smooth out the faint end

of the source distribution. The simplest way to cure this is to just introduce a lower cutoff flux F_{min} below which no sources contribute, and since we are mainly interested on the effects of the bright end of the distribution, our main conclusions will be independent of the particular way in which this cutoff is handled.

Another simple scenario which has been considered is that the CR sources are transient, such as in the models of acceleration during GRBs. In this case, due to the energy dependent time delays $\tau(E, d)$ suffered by CRs after traversing a distance d across a magnetised universe, a bursting source will be seen (neglecting energy losses and strong lensing effects) as a monochromatic flux at the observer, with an energy slowly decreasing with time but on a scale typically much longer than the duration of the experiments [13]. However, stochastic energy losses during CR propagation introduce a spread in time delays $\Delta\tau(d, E)$ which leads to the observation of CRs with a certain spread of energies at any given time, with $\Delta E/E \sim \Delta\tau/\tau$. Moreover, when strong magnetic lensing effects are present, so that a CR source is actually observed as a very large number of multiple images associated to different alternative paths from the source to the observer, this also introduces a spread in the energies of the particles observed at any given time. There are two ways in which these processes affect the number of sources above a given flux⁶ which can be observed at any given moment. First, the longer is the spread in time delays, the more likely it becomes for a source to contribute to the CR fluxes during the period of observation, but however since the CRs produced in the burst will spread over a longer time interval, the flux will be more suppressed than the naive d^{-2} behaviour. As argued in ref. [13], one expects $\Delta\tau \propto \tau \propto (d/E)^2$, and hence one has that $F \propto 1/(d^2\Delta\tau) \propto d^{-4}$. Hence, the number of sources above a certain flux (i.e. within an associated distance $d \propto F^{-1/4}$) will be [13]

$$n_s(> F, E) \propto \frac{4}{3}\pi d^3 \Delta\tau \propto F^{-5/4}. \quad (20)$$

This gives a differential source density

$$\frac{dn_s}{dF} \propto F^{-9/4}. \quad (21)$$

In view of the previous results, we may then parametrise the source distribution with a simple power law

$$\frac{dn_s}{dF} = \frac{\alpha N_s}{F_{min}} \left(\frac{F_{min}}{F} \right)^{\alpha+1}, \quad (22)$$

with a lower cutoff at the minimum flux F_{min} and where N_s is the total number of sources above F_{min} . For the steady source model one has $\alpha = 3/2$ while for the bursting scenario $\alpha = 5/4$. For these simple scenarios one obtains, from eqs. (16) and (17), an expected average number of multiplets

$$\overline{N}_m = \frac{\alpha N_s}{m!} \Gamma(m - \alpha, F_{min}\mathcal{E}) (F_{min}\mathcal{E})^\alpha \quad (23)$$

⁶For transient sources, the flux should be considered in a given energy bin around E [13].

with $\Gamma(x, y)$ the incomplete Gamma function. Since we are interested in cases where $1 < \alpha < 2$, one finds that as long as $\mathcal{E} \ll F_{min}^{-1}$ (i.e. that the faint sources have a small probability of leading to one event) the expected average number of event clusters (with $m \geq 2$) will have very little sensitivity to the second argument of the Gamma function, leading to $\bar{N}_m \propto \mathcal{E}^\alpha \Gamma(m - \alpha)/m!$, while the number of single events (not in clusters) does depend on the faint end of the source distribution⁷, having the approximate behaviour $\bar{N}_1 \simeq \alpha N_s \mathcal{E} F_{min}/(\alpha - 1)$. Clearly these approximate behaviours cease to be valid when $\mathcal{E} \simeq F_{min}^{-1}$, but before that happens (as should be anyway the case for the next few years) one has that while the average number of individual events (which will be the majority) should grow approximately like \mathcal{E} , the number of clusters grows at a faster rate $\bar{N}_m \propto \mathcal{E}^\alpha$. Of course the total number of events is expected to grow strictly proportionally to the exposure, as results from Eq. (16), since $\bar{n} \equiv \sum m \bar{N}_m = F_{tot} \mathcal{E}$, with F_{tot} the total flux. The fraction of events which are in multiplets (neglecting here chance coincidences) grows hence, as long as $\mathcal{E} \ll F_{min}^{-1}$, as $\mathcal{E}^{\alpha-1}$.

It is also interesting to compute the ratio of expected number of clusters with different multiplicities,

$$\frac{\bar{N}_l}{\bar{N}_m} \simeq \frac{m!}{l!} \frac{\Gamma(l - \alpha)}{\Gamma(m - \alpha)} \quad (l, m \geq 2), \quad (24)$$

and in particular for $l = m + 1$ one obtains

$$\frac{\bar{N}_{m+1}}{\bar{N}_m} \simeq \frac{(m - \alpha)}{(m + 1)} \quad (m \geq 2). \quad (25)$$

Another related result is that

$$\frac{\sum_{m=3}^{\infty} \bar{N}_m}{\bar{N}_2} \simeq \sum_{m=3}^{\infty} \prod_{l=3}^m \frac{(l - 1 - \alpha)}{l}. \quad (26)$$

Notice that these ratios are independent of the total number of events \bar{n} , contrary to the case of chance coincidences. On the other hand, the dependence on the distribution of the source fluxes is rather noticeable, for instance, for $\alpha = 3/2$ the ratio in eq. (26) is 0.33, while for $\alpha = 5/4$ it becomes instead 0.60.

All these statistical quantities do not depend on whether the angular distribution of sources in the sky is isotropic or structured, as long as the average radial distribution does not differ much from uniformity. Of course fluctuations would affect these average behaviours, and they could come from a spread in the source luminosities, which could be either intrinsic or caused by magnetic lensing effects [17] (this

⁷Since our treatment of the faint end has been rather crude, one should not use statistics such as the number of single vs. double events to get information on the number of sources contributing, and in this respect the parameter N_s just comes out as a normalisation constant. An estimate of the number of sources producing CRs depends sensitively on the way the faint end is handled, and will require other general features of the CR sources, such as the luminosity distribution, to be understood as well [12, 14, 15, 16].

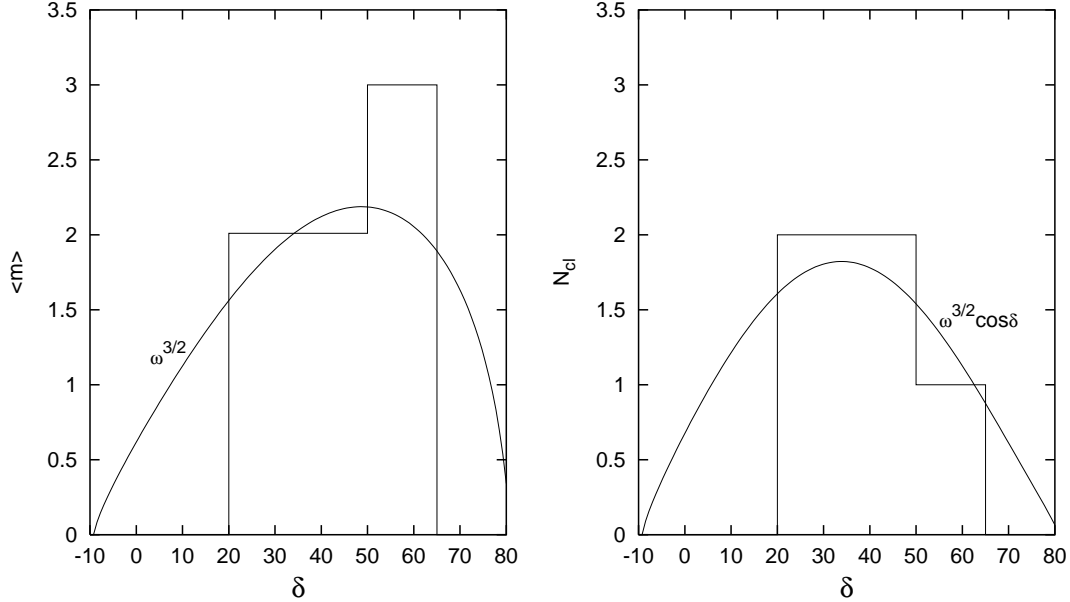


Figure 4: Distribution in declination of cluster multiplicity (left panel) and number of clusters (right panel) in AGASA data (histograms) compared to that expected from an isotropic distribution of stationary sources ($\alpha = 3/2$, see text), for which the overall normalization adopted is just arbitrary (solid curves).

could typically produce some clusters of larger than expected multiplicities), from fluctuations in the radial source density distribution, from small statistics, etc..

Regarding the effects of varying exposures, it is clear that in the regions of larger exposures the sources are expected to yield clusters of larger multiplicities on average, so that one expects that with large statistics, an uniform distribution of sources would lead to an average multiplicity varying as $\omega(\delta)^\alpha$. On the other hand, the number of clusters (with multiplicities $m \geq 2$), i.e. $N_{cl} = \sum_{m \geq 2} \bar{N}_m$, should follow the distribution $dN_{cl} \propto \omega(\delta)^\alpha \cos \delta d\delta$, and although the data are still scarce, the observed clusters are consistent with these behaviours, as illustrated in Figure 4. Notice that the total number of events (in clusters or not) should follow $dn \propto \omega(\delta) \cos \delta d\delta$ if the source distribution is isotropic, so that a deviation from this behaviour would be a clear signal of anisotropies, no matter what is the underlying reason for the clustering observed (i.e. chance coincidences vs. strong sources).

4 Nearest neighbour distribution

Up to now we have discussed in detail the properties of the distribution of multi-plets in the different possible clustering scenarios. One of the main criticisms to the statistics discussed has been the dependence on the angular binning of the data, as the results depend on its choice. We will discuss now another statistics to analyse small scale clustering, the frequency distribution of the angular distance to the nearest neighbours of each event, which avoids this problem. Each event has a first, a second, and so on, nearest neighbour event, and the idea is to look at the distribution of their distances. This statistics has some advantages over the autocorrelation function of pairs when studying non-linear clustering, as it depends on the correlation functions of all orders. This is because the probability of finding no events at a distance smaller than a given angle depends on the correlation functions of all orders. This method has been used for example by Bahcall and Soneira to study the distribution of stars and the fraction of binaries and triples [18].

The cumulative distributions of the distance to the first and second neighbour for the 57 events of AGASA as a function of the angular distance are shown in the solid histogram of Figure 5. The expected distribution for a sample of random points in the sphere has been computed by Scott and Stout [19]. However, in order to compare with the distribution of the AGASA data we have to take into account the incomplete sky coverage and inhomogeneous exposure. Thus, we used instead the results of 10000 simulations of 57 random events with the AGASA exposure, the mean of which is shown in Figure 5 (dashed line). The AGASA distribution shows an excess of first neighbours at small angles, with a maximal departure at 2.5° , with the excess disappearing at angles slightly larger than 5° . This excess is clearly related to the excess of doublets and triplets at small angles discussed before. The cumulative histogram of the second neighbours (dotted histogram) also shows an extended excess with respect to random expectations (dash-dotted line) from angles around 2.5° up to 15° , with a maximal deviation at 11° .

In order to have a measure of the significance of the first and second neighbour excesses, the natural choice would be to perform a Kolmogorov-Smirnov test. However, a necessary condition for this test is that the data be all independent, and the nearest neighbour separations between events are not independent variables (since often the nearest neighbour of an event has as nearest neighbour that event). Thus, we determine the significance of a given deviation D of the cumulative histogram from that expected from a random sample of the same number of events using Monte-carlo simulations and look for the fraction of the simulations with a deviation from the mean larger than the observed D . The first neighbour distribution shows a maximum deviation from the mean of the random simulations $D = 0.146$, with 6% of the simulations having larger deviations at any angle, while the second neighbours curve maximum deviation is $D = 0.246$, with 0.8% of the simulations showing larger deviations.

We have also checked the deviation of the mean angular separation to the first

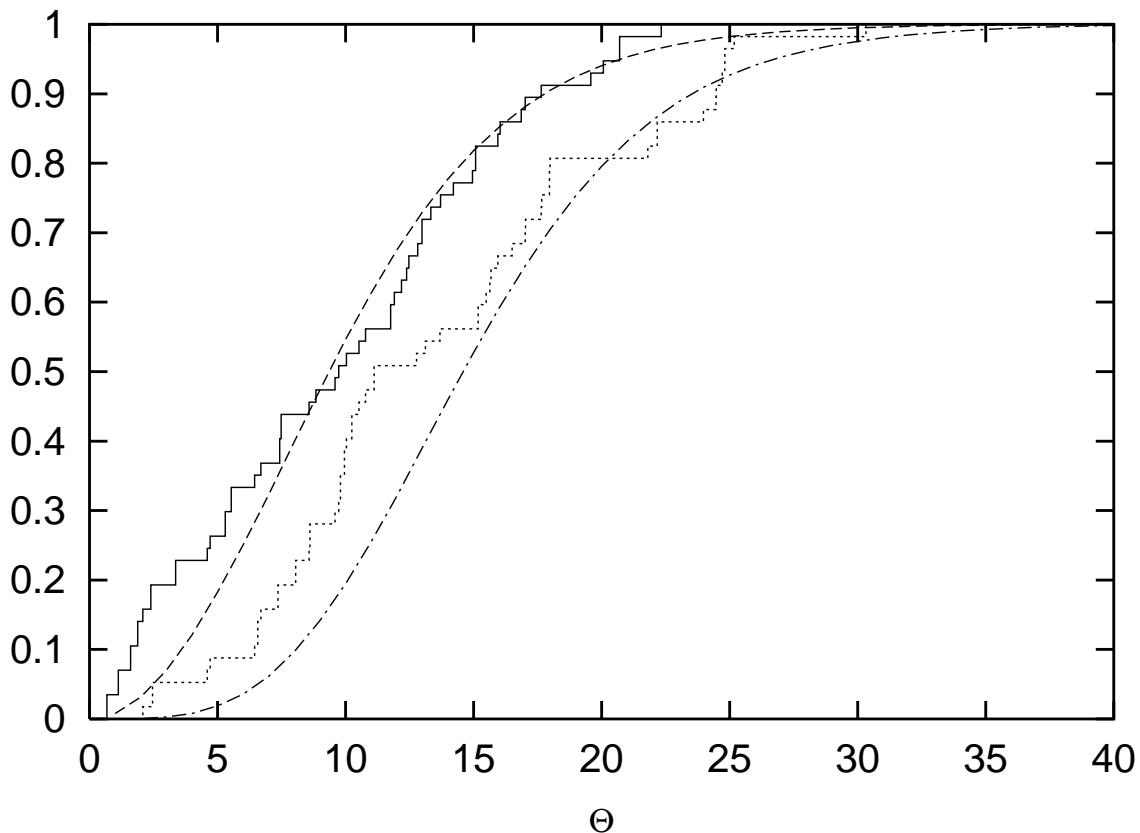


Figure 5: Cumulative distribution of the distance to the first (solid histogram) and second (dotted histogram) neighbour of the 57 AGASA events above 4×10^{19} eV. The dashed and dashed-dotted curves are the mean distributions for 10000 random realizations of 57 events with AGASA exposure.

and second neighbour of the data from that expected for a random sample. While the AGASA data have first neighbour mean distance $\langle \theta_1 \rangle_{AG} = 9.66^\circ$, the mean for a random sample is $\langle \theta_1 \rangle_{ran} = 10.18^\circ$, with 25% of the simulations having values smaller than the AGASA one. For the second neighbours we find $\langle \theta_2 \rangle_{AG} = 13.57^\circ$, while $\langle \theta_2 \rangle_{ran} = 15.35^\circ$, with only 2.3% of the simulations having smaller than AGASA's mean value.

Let us note that the maximum deviation of the second neighbour distance cumulative distribution, that takes place at $\theta \simeq 11^\circ$, reflects the clustering at all smaller scales. In particular, the effect of the triplet is clearly seen in the rise of the histogram at 2.5° , which produces a shift in the whole curve. Also the excess of doublets at small angles is expected to affect the second neighbours distance distribution: the events entering in the doublets will have their second neighbours at the mean distance at which singlets have their first neighbours. Then, we may ask if the whole deviation of the second neighbours at 11° can be explained as a

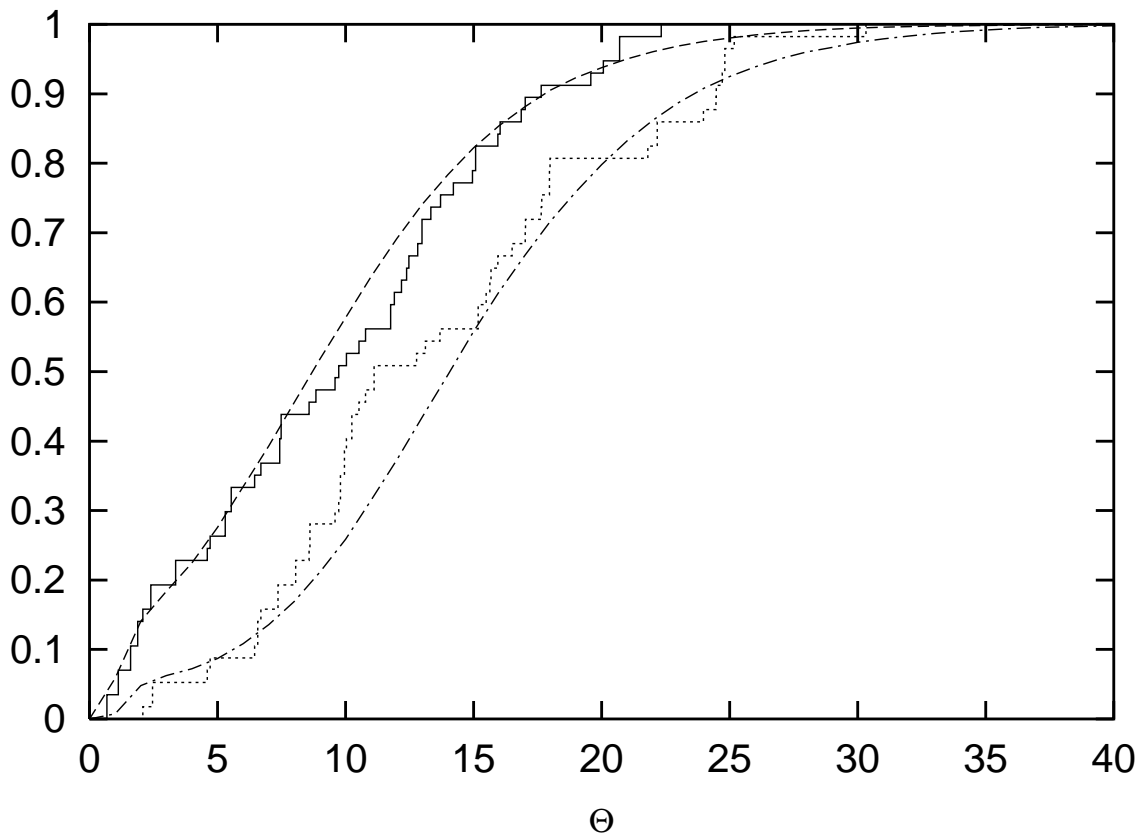


Figure 6: Same as Figure 5, but now the simulations have 53 events randomly thrown with AGASA exposure, and the remaining 4 events are forced to form one triplet and two doublets within 2.5° of the rest.

result of the excess of small scale clustering (triplet and doublets). To answer this, we performed a similar analysis, comparing the data with 10000 simulations of 57 events, 53 of which are randomly thrown with the AGASA exposure, and the rest are forced to form a triplet and two doublets within 2.5° with some of the other events (chance alignments of random points are expected to produce 1.5 additional doublets on average at 2.5°). The resulting cumulative distributions for the first and second neighbours distance are shown in Figure 6. The first neighbours distribution of the AGASA data are now in good agreement with the result of the simulations, as well as the small angle piece of the second neighbours distribution. There remains however a deviation of this distribution with a maximum distance $D = 0.187$ at 11° , with 7.6% of the simulations showing larger deviations. The mean distance to the second neighbour of the simulation is now reduced to $\langle \theta_2 \rangle_{ran} = 14.5^\circ$, with 15% of the simulations showing values smaller than the AGASA's one. While the significance of the deviation is reduced by forcing the small scale clustering in the simulations, it remains however a hint of extra clustering at angular scales around 10° that may be due to point source events that have been deflected by magnetic

fields, or to structure in the spatial distribution of sources.

5 Discussion

We have seen that the statistics of clusters of events with different multiplicities is a very useful tool that may help characterise the nature of UHECR sources. We have analysed the way in which the relative number of clusters with different multiplicities, their change with increasing exposure, and their distribution with declination can help discriminate among alternative source scenarios. In particular, one of the most striking differences between the individual sources and chance coincidences scenarios for clustering is the expected hierarchy of the number of clusters with different multiplicities. For example, the ratio between the number of triplets or higher multiplets and doublets is $\sim 1/3$ for the steady source model (or 0.6 for the bursting one), while it is only $\sim n/3N$ for the chance coincidences, where $N \sim 10^3(2.5^\circ/\theta)^2$. In case the clusters are dominated by individual sources, we see that with significant statistics this may even give a handle to discriminate between bursting and steady source scenarios. Moreover, the evolution of this ratio (which is proportional to the exposure for chance coincidences, while independent of it for individual sources) will give a further tool to discriminate among scenarios. On the other hand, the relative fraction of events in clusters (with respect to the unclustered ones) is only $\sim n/2N$ for the chance coincidences of an isotropic distribution, but could be significantly enhanced if the distribution of sources is anisotropic. This should be however testable by studying the overall event distribution once larger statistics are achieved. In the case of clusters produced by individual sources, this fraction depends instead sensitively on the amount of very faint sources present.

We have applied our analysis to the published set of 57 AGASA events above 4×10^{19} eV just for illustrative purposes, since it is clearly insufficient to draw definitive conclusions. Nevertheless, our results indicate that a modest increase in the number of events may already give much stronger hints about the source properties. In this respect, even the release of the latest AGASA data, which represents a 50% increase with respect to the published data, could have some impact. For instance, it would be natural to expect that the triplet becomes a quadruplet, and some doublets become triplets, if they are due to individual sources, while this would be very unlikely if they arose from chance coincidences.

We have also applied an alternative statistical tool to analyse UHECR clustering: the nearest neighbour distribution. It has the advantage over the pair autocorrelation method of being less sensitive to binning, and that it depends not just on the pair correlations but on correlations to all orders [20]. Applied to AGASA data, it gives an alternative measure of the small angular scale clustering, and also points out to an excess of clustering with respect to random expectations which persists up to 15° , that manifests in the second neighbours cumulative distribution (Figure 5), and which is also hinted by the defect of doublets and excess of triplets at scales up to

15° in Figure 1. Angular spread of events in a cluster due to deflections by magnetic fields, and structure in the spatial distribution of sources, are among conceivable causes of such signal, which should be looked upon with better statistics.

Acknowledgments

Work supported by ANPCyT, CONICET, Fundación Antorchas and the Guggenheim Foundation.

References

- [1] J. W. Cronin, *The highest-energy cosmic rays*, talk presented at TAUP 2003, Seattle, USA, astro-ph/0402487.
- [2] M. Takeda et al., *Small scale anisotropy of cosmic rays above 10^{19} eV observed with the Akeno Giant Air Shower Array*, *Astrophys. J.* **522** (1999) 225, astro-ph/9902239; M. Teshima et al., *The arrival direction distribution of extremely high energy cosmic rays observed by AGASA*, Proc. 28th ICRC, Tokyo (2003), 437, Universal Academy Press, Inc.
- [3] Y. Uchihori, M. Nagano, M. Takeda, M. Teshima, J. Lloyd-Evans and A.A. Watson *Cluster analysis of extremely high-energy cosmic rays in the northern sky*, *Astropart. Phys.* **13** (2000) 151, astro-ph/9908193.
- [4] R.U. Abbasi et al., *Study of small-scale anisotropy of ultrahigh energy cosmic rays observed in stereo by HiRes*, astro-ph/0404137.
- [5] P. Sommers, *Cosmic ray anisotropy analysis with a full-sky observatory*, *Astropart. Phys.* **14** (2001) 271, astro-ph/0004016.
- [6] P.G. Tinyakov and I.I. Tkachev, *Correlation function of ultrahigh energy cosmic rays favors point sources*, *Sov. Phys. JETP Lett.* **74** (2001) 1, astro-ph/0102101.
- [7] N.W. Evans, F. Ferrer and S. Sarkar, *Clustering of ultrahigh-energy cosmic rays and their sources*, *Phys. Rev. D* **67** (2003) 103005, astro-ph/0212533.
- [8] C. B. Finley and S. Westerhoff, *On the evidence for clustering in the arrival directions of AGASA's ultrahigh energy cosmic rays*, astro-ph/0309159.
- [9] H. Goldberg and T. J. Weiler, *Clustering in highest energy cosmic rays: physics or statistics?*, *Phys. Rev. D* **64** (2001) 056008, astro-ph/0009378.
- [10] G. Medina-Tanco, *Ultra-high energy cosmic rays: are they isotropic?*, *Astrophys. J.* **549** (2001) 711, astro-ph/0009336.

- [11] E. Waxman, K. B. Fisher and T. Piran, *The signature of a correlation between cosmic ray sources above 10^{19} eV and large-scale structure*, *Astrophys. J.* **483** (1997) 1, astro-ph/9604005.
- [12] S. L. Dubovsky, P. G. Tinyakov and I. I. Tkachev, *Statistics of clustering of ultra-high energy cosmic rays and the number of their sources*, *Phys. Rev. Lett.* **85** (2000)1154, astro-ph/0001317.
- [13] J. Miralda-Escudé and E. Waxman, *Signatures of the origin of high-energy cosmic rays in cosmological gamma-ray bursts*, *Astrophys. J.* **462** (1996) L59, astro-ph/9601012.
- [14] Z. Fodor and S. D. Katz, *Ultra high energy cosmic rays from compact sources*, *Phys. Rev. D* **63** (2001) 023002, hep-ph/0007158.
- [15] C. Isola and G. Sigl, *Large scale magnetic fields and the number of cosmic ray sources above 10^{19} eV*, *Phys. Rev. D* **66** (2002) 083002, astro-ph/0203273.
- [16] P. Blasi and D. De Marco, *The small scale anisotropies, the spectrum and the sources of ultrahigh-energy cosmic rays*, *Astropart. Phys.* **20** (2004) 559, astro-ph/0307067.
- [17] D. Harari, S. Mollerach and E. Roulet, *Signatures of galactic magnetic lensing upon ultra high energy cosmic rays*, *JHEP* **08** (1999) 022; D. Harari, S. Mollerach, E. Roulet and F. Sánchez, *Lensing of ultra high energy cosmic rays in turbulent magnetic fields*, *JHEP* **03** (2002) 045.
- [18] J. N. Bahcall and R. M. Soneira, *The distribution of stars to $V=16$ th magnitude near the north galactic pole: normalization, clustering properties, and counts in various bands*, *Astrophys. J.* **246** (1981) 122.
- [19] D. Scott and C. A. Tout, *Nearest neighbour analysis of random distributions on a sphere*, *Mon. Not. Royal Astron. Soc.* **241** (1989) 109.
- [20] S. D. M. White, *The hierarchy of correlation functions and its relation to other measures of galaxy clustering*, *Mon. Not. Royal Astron. Soc.* **186** (1979) 145.